

# A Small Molecule Promotes Mitochondrial Fusion in Mammalian Cells\*\*

Danling Wang, Jianing Wang, Ghislain M. C. Bonamy, Shelly Meeusen, Richard G. Brusch, Carolina Turk, Pengyu Yang, and Peter G. Schultz\*

Mitochondria are highly dynamic cellular organelles that continuously undergo fission and fusion.<sup>[1]</sup> This dynamic nature plays a key role in regulating mitochondrial function, and also gives mitochondria their heterogeneous morphology.<sup>[2]</sup> Disruption of the balance between mitochondrial fusion and fission, especially a shift towards fission, contributes to a variety of human disorders, including neurodegenerative disease, metabolic disease, and ischemia.<sup>[3]</sup> In addition, fragmented mitochondria are early signs of activation of apoptosis,<sup>[4]</sup> and fusion of mitochondria by genetic or chemical manipulation has been shown to have an anti-apoptotic effect.<sup>[5]</sup> Thus, the identification of small molecules that modulate mitochondrial dynamics can provide useful tools to study mitochondrial function and may ultimately lead to new therapeutics. Here, we report the identification and preliminary biological characterization of the small molecule, M1, which significantly restores the mitochondrial tubular network in response to genetically or chemically induced fragmentation.

Mitochondrial fusion is a two-step process in which the outer and inner mitochondrial membranes (OMM and IMM, respectively) fuse separately, but in an ordered fashion.<sup>[6]</sup> The core components of the mitochondrial fusion machinery are the OMM proteins, mitofusin 1 and 2 (Mfn1 and Mfn2), and the IMM protein, optic atrophy 1 (Opa1).<sup>[7]</sup> Unlike

wild-type mouse embryonic fibroblasts (WT MEFs), which mainly have interconnected tubular mitochondria, Mfn1 Knockout (KO) MEFs exhibit severely and uniformly frag-

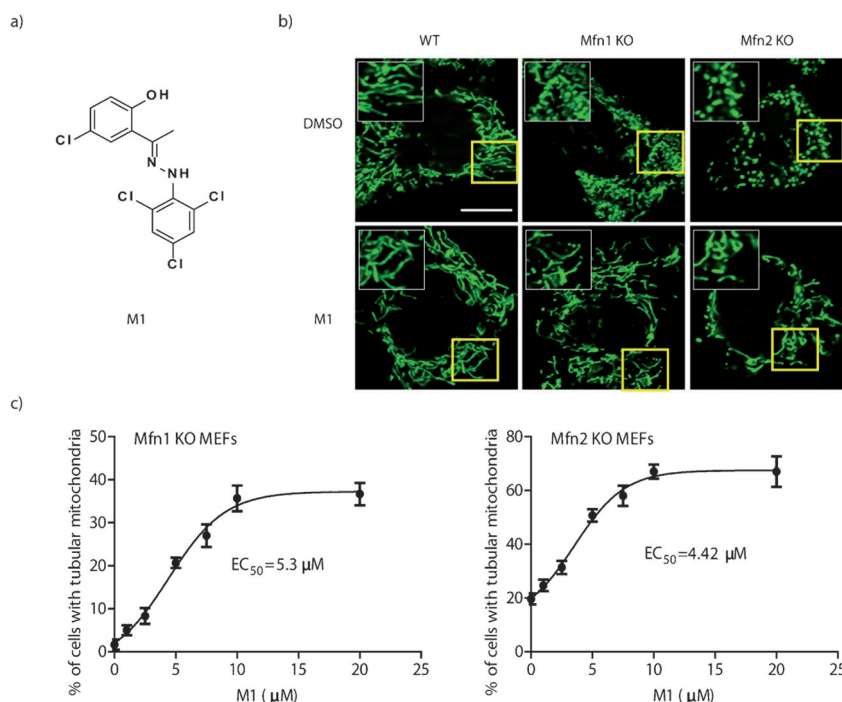


**Figure 1.** M1 induces mitochondrial elongation. a) Chemical structure of M1. b) Confocal microscopic analysis of mitochondria in WT, Mfn1 KO and Mfn2 KO MEFs. Cells were treated with 0.1% DMSO control (top panels) or 5 μM M1 (bottom panels) for 24 h, followed by labeling with 500 nm Mito Tracker Green and imaging with a Leica 710 confocal microscope. The white box depicts a higher magnification of the yellow boxed region. Scale bar: 10 μm. c) Percentage of cells with tubular mitochondria (> 5 μm) in Mfn1 KO MEFs (left panel) and Mfn2 KO MEFs (right panel) after incubation with different concentrations of M1 for 24 h.

[\*] Dr. D. Wang, Dr. J. Wang, Dr. P. Yang, Prof. Dr. P. G. Schultz  
Department of Chemistry, the Scripps Research Institute  
10550 North Torrey Pines Road, La Jolla, CA 92037 (USA)  
E-mail: schultz@scripps.edu  
Homepage: <http://schultz.scripps.edu/>

Dr. G. M. C. Bonamy, Dr. S. Meeusen, R. G. Brusch, C. Turk  
Genomics Institute of the Novartis Research Foundation  
10675 John J. Hopkins Dr, San Diego, CA 92121 (USA)

[\*\*] We acknowledge financial support from the Skaggs Institute for Chemical Biology (to P.G.S.). We thank Dr. Shoutian Zhu and Dr. Kristen Johnson for helpful discussion and critical reading of the manuscript.

Supporting information for this article is available on the WWW under <http://dx.doi.org/10.1002/anie.201204589>.

fragmented mitochondria in the shapes of small spheres or very short rods (less than 5 μm).<sup>[8]</sup> Using the mitochondria-selective fluorescent dye, Mito Tracker, we developed an image-based high-throughput screen to monitor mitochondrial fusion (see Material and Methods section in the Supporting Information). Approximately 75000 compounds from several commercially available compound libraries, including Maybridge, LOPAC and TOCO, were screened for their ability to rescue mitochondrial fragmentation in Mfn1 KO MEFs; 17 compounds were confirmed to be active in a dose-dependent manner (see Table S1 in the Supporting Information). It is interesting to note that multiple hits contain either a hydrazone or acylhydrazone moiety. Mfn1

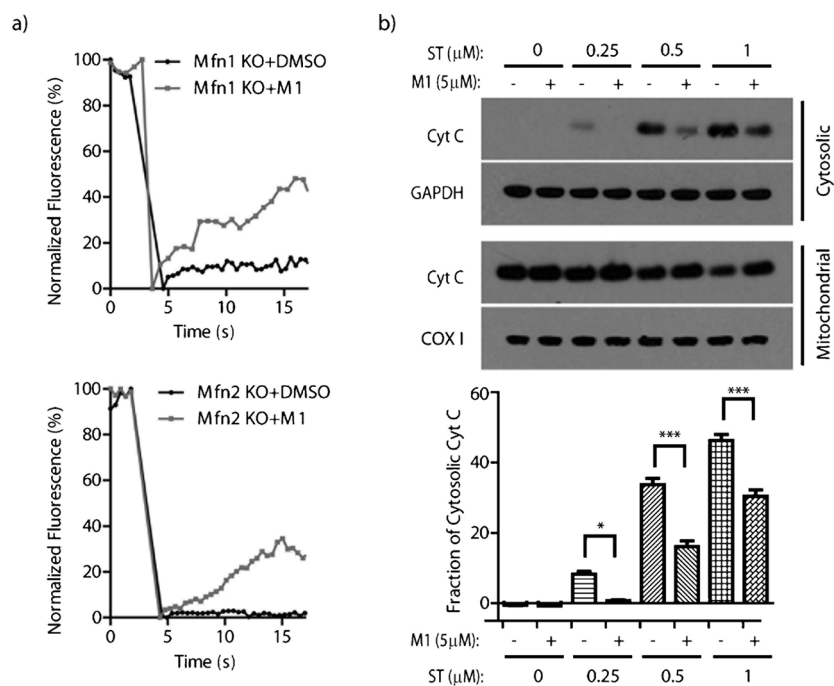


**Figure 2.** M1 increases mitochondrial connectivity and integrity. a) Mitochondrial network connectivity in Mfn1 KO MEFs or Mfn2 KO MEFs. Cells transfected with mito-GFP were treated with 0.1 % DMSO control or 5  $\mu$ M M1 for 24 h before the FRAP assay at 37°C. Defined  $2 \times 2 \mu\text{m}^2$  regions of interest (ROI) were bleached with a 488 nm laser line and the recovery of mito-GFP fluorescence was monitored over 30 cycles of imaging with about 0.5 s interval. The curve represents an average of 20 individual FRAP curves. b) HeLa cells were pre-incubated with 0.1 % DMSO control or 5  $\mu$ M M1 for 24 h before treatment with 0, 0.25, 0.5, or 1  $\mu$ M staurosporine (ST) for 2 h. Cytosolic and mitochondrial fractions were subjected to Western blot analysis for the detection of CytC using anti-CytC antibody. GAPDH and COX I were used as loading controls for each fraction (upper panels). Cytosolic Cyt C was quantified by calculating the percentage of cytosolic Cyt C band intensity over mitochondrial plus cytosolic Cyt C band intensities after normalization with loading controls. \*  $p < 0.05$ . \*\*\*  $p < 0.001$ .

and Mfn2 are highly homologous, and both are located in the OMM. They possess both partially redundant and distinct activities and act mainly as homotypic and heterotypic complexes to promote mitochondrial fusion.<sup>[9]</sup> 15 out of 17 active compounds also improved the mitochondrial fragmentation phenotype in Mfn2 KO MEFs, indicating a more general phenotypic association of these compounds rather than an association with any specific gene.

The most active compound, hydrazone M1 (Figure 1 a), was chosen for further study. M1 dose-dependently induced mitochondrial elongation in both Mfn1 KO MEFs and Mfn2 KO MEFs (Figure 1 b), with half maximal effective concentrations ( $\text{EC}_{50}$  values) of 5.3 and 4.42  $\mu$ M, respectively (Figure 1 c). However, when Mfn1/2 double KO (DKO) or Opa1 KO MEFs were treated with M1, no mitochondrial elongation activity was observed (see Figure S1 in the Supporting Information). This result suggests a requirement for basal fusion activity for M1 to elongate mitochondria. Unlike stress-induced mitochondrial hyperfusion, which shows dramatically elongated mitochondria, even in WT cells,<sup>[7b]</sup> M1 appears to selectively affect cells with fragmented mitochondria, as incubation with M1 did not lead to a significant

change of mitochondrial morphology in WT MEFs (Figure 1 b). The mitochondrial elongation effects of M1 were further examined using transmission electron microscopy (TEM).<sup>[10]</sup> Small spherical mitochondria ( $\leq 1 \mu\text{m}$  length), but few tubular mitochondria ( $\geq 5 \mu\text{m}$  length), are found in Mfn1 KO MEFs. After treatment with M1, tubular mitochondria ( $\geq 5 \mu\text{m}$  length) are readily observed (Figure S2a, quantified in Figure S2b). In addition, we also examined the morphologies of the endoplasmic reticulum (ER) and lysosomes in Mfn1 KO cells after M1 treatment. Neither of these organelles displayed obvious morphological changes (Figure S3), suggesting that the elongation effect of M1 is mitochondria specific.

Mitochondrial elongation can result from either increased fusion or decreased fission activity.<sup>[11]</sup> To distinguish between these possibilities, we first evaluated fusion activity by measuring mitochondrial connectivity using a fluorescence recovery after photobleaching (FRAP) assay.<sup>[5b,12]</sup> Upon treatment with M1, both Mfn1 KO MEFs and Mfn2 KO MEFs displayed faster recoveries of mitochondrial matrix-targeted green fluorescent protein (mito-GFP) in mitochondria disconnected from the network, suggesting increased fusion of mitochondrial structures from the surrounding unbleached area (Figure 2 a). As expected, in Mfn1/2 DKO MEFs and Opa1 KO MEFs, which are deficient in fusion capacity, there was no enhancement of fusion activity by M1 (Figure S4). Next, we investigated the

effect of M1 on fission activity. Peroxisomes and mitochondria use different proteins for fusion, but share key components of the fission machinery, including Drp1, Fis1, and Mff.<sup>[13]</sup> We therefore asked whether M1 affects peroxisomal fission, but saw no obvious effects on the peroxisomal morphology (Figure S5). Taken together, these results suggest that M1 induces mitochondrial elongation by enhancing fusion activity instead of inhibiting fission.

To further investigate the mechanism underlying the effects of M1, we systematically assayed the expression of the proteins and genes known to be involved in regulating mitochondrial dynamics, including Mfn1, Mfn2, Opa1, Drp1, Fis1, PGC-1 $\alpha$ , PGC-1 $\beta$ , PPAR- $\gamma$ , and ERR $\alpha$ .<sup>[14]</sup> (Figure S6). Surprisingly, we noted that steady-state levels of Mfn1 were significantly reduced in Mfn2 KO MEFs, raising the possibility that M1 may rescue an Mfn1 fusion deficiency in both lines. Interestingly, we found that the  $\alpha$  and  $\beta$  subunits of mitochondrial adenosine triphosphatase (ATP) synthase (ATP5A and ATP5B, respectively) are down-regulated in Mfn1 and Mfn2 KO MEFs. In the presence of M1, the levels of both proteins return to those in WT MEFs (Figure 3 a). Moreover, overexpression of ATP5A, ATP5B, or both

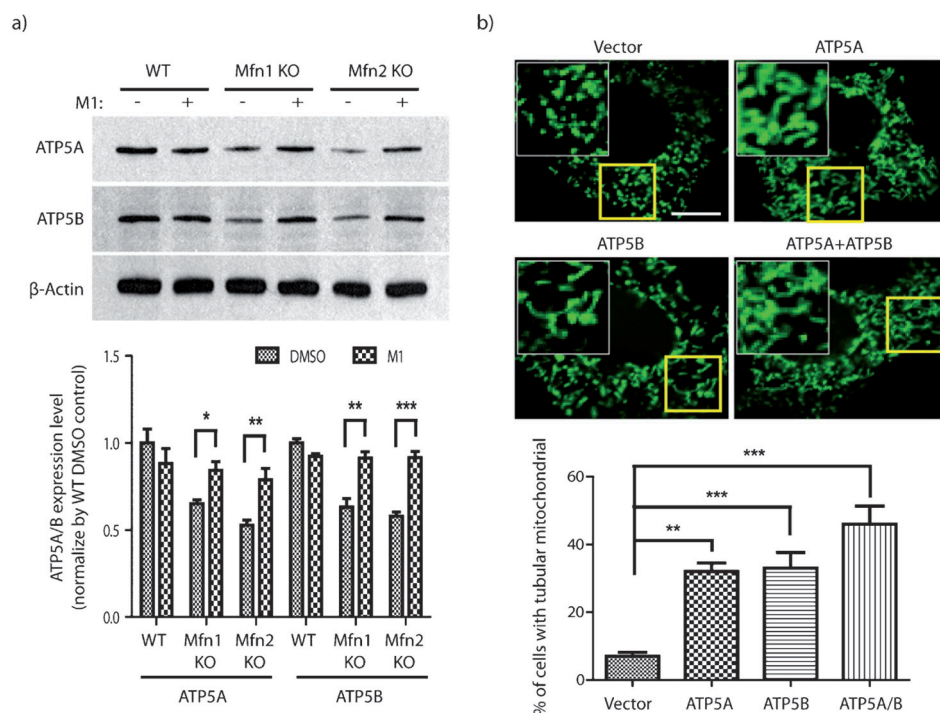


**Figure 3.** M1 increases ATP5A/B protein levels. a) Western blot analysis of ATP5A and ATP5B in WT, Mfn1 KO and Mfn2 KO MEFs after incubation with 0.1 % DMSO control or 5  $\mu$ M M1 for 24 h. For details see the Experimental Section. b) Confocal microscopic analysis of mitochondria in Mfn1 KO MEFs after overexpression of ATP5A or ATP5B or both. For details see the Experimental Section. The white box depicts a higher magnification of the yellow boxed region. Scale bar: 10  $\mu$ m. Quantification of the percentage of cells that showed tubular mitochondria (> 5  $\mu$ m). More than 100 cells per group were evaluated (lower panel, \*\*  $p < 0.01$ ; \*\*\*  $p < 0.001$ )

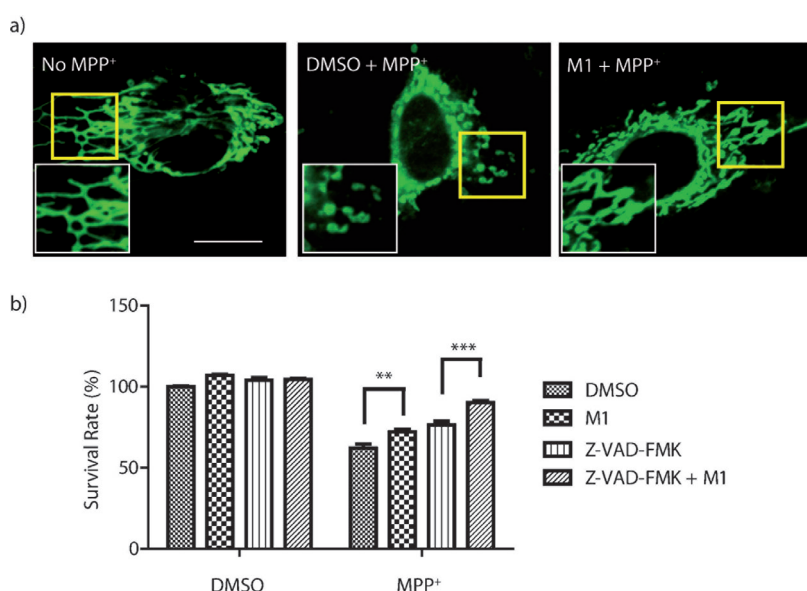


**Figure 4.** M1 protects SH-SY5Y cells from MPP<sup>+</sup> induced mitochondrial fragmentation and cell death. a) Confocal microscopic analysis of mitochondria in SH-SY5Y after Mito Tracker Green fluorescence labeling. SH-SY5Y cells were pre-treated with 0.1 % DMSO control (top middle panel) or 5  $\mu$ M M1 (top right panel) for 24 h followed by 4 h treatment with 125  $\mu$ M MPP<sup>+</sup>. Scale bar: 10  $\mu$ m. b) Cellular survival was measured by the MTT assay. SH-SY5Y cells were treated with or without 125  $\mu$ M MPP<sup>+</sup> in the presence or absence of 5  $\mu$ M M1 and 1  $\mu$ M Z-VAD-FMK (\*\*  $p < 0.01$ , \*\*\*  $p < 0.001$ ).

(ATP5A/B) in Mfn1 KO MEFs with recombinant DNA replicated the phenotype of M1 treatment, with an increased percentage of cells showing interconnected tubular mitochondria (> 5  $\mu$ m; Figure 3b and Figure S7). Furthermore, inhibition of ATPase by oligomycin significantly blocked the mitochondrial fusion activity of M1 in Mfn1 KO MEFs (Figure S8a, quantified in Figure S8b). Treatment of WT MEFs with oligomycin also resulted in a profound mitochondrial fragmentation phenotype (Figure S9). These data suggest that M1 promotes mitochondria fusion by increasing the expression levels of ATP5A/B. ATP5A/B are the two major components of the catalytic center of ATP synthase (mitochondrial complex V). Although it has long been speculated that ATPase proteins play essential roles in mitochondrial cristae formation in yeast, their involvement in dynamic regulation is not clear.<sup>[15]</sup> Our results support an important role for these proteins

in mitochondria dynamics. Recently, mitochondrial fragmentation and dysfunction have been reported in patient fibroblasts carrying a mitochondrial complex V deficient mutation,<sup>[16]</sup> which is consistent with our findings.

Aberrations in mitochondrial dynamics are associated with various human diseases. For example, 1-methyl-4-phenyl-pyridinium (MPP<sup>+</sup>) associated neuronal toxicity is implicated in Parkinson's disease (PD) pathogenesis and suggested to involve mitochondrial fragmentation and dysfunction.<sup>[17]</sup> We therefore investigated the ability of M1 to prevent MPP<sup>+</sup> induced cytotoxicity of dopaminergic SH-SY5Y neuroblastoma cells, a widely used in vitro model for PD. Treatment with M1 significantly inhibited MPP<sup>+</sup> induced mitochondrial fragmentation, as evidenced by elongated mitochondrial structures compared to dimethyl sulfoxide (DMSO) control (Figure 4a), and resulted in a higher neuronal survival rate (Figure 4b). When combined with the pan caspase inhibitor Z-VAD-FMK at a relatively low concentration (1  $\mu$ M), M1 showed a synergistic effect in protecting SH-SY5Y cells from cell death (Figure 4b). Moreover, when treated with the apoptosis inducer

staurosporine (ST), M1 pre-treated cells showed significantly decreased Cyt C release and a higher survival rate (Figure 2b and Figure S10), consistent with reduced mitochondrial fragmentation and release of CytC into the cytosol, a key step in caspase activation and the initiation of apoptosis.<sup>[5a,18]</sup> These data suggest that M1, by itself or in combination with other protective agents, improves cell survival through increased mitochondria fusion.

In conclusion, we have identified a small molecule from a phenotypic image-based screen that promotes the fusion of fragmented mitochondria and protects cells from mitochondrial fragmentation associated cell death. Further investigation is required to decipher the molecular mechanisms by which M1 regulates ATP5A/B protein levels and mitochondria fusion/fission dynamics. This work may ultimately lead to a new approach to the treatment of diseases associated with mitochondrial dysfunction.

## Experimental Section

For the Western blot analysis (see Figure 3a)  $\beta$ -actin was used as a loading control (upper panel). Quantification of each band was determined using ImageJ software. ATP5A and ATP5B band intensities were normalized by  $\beta$ -actin controls (lower panel, \*  $p < 0.05$ ; \*\*  $p < 0.01$ ; \*\*\*  $p < 0.001$ ).

For the confocal microscopic analysis (see Figure 3b) of mitochondria the Mfn1 KO MEFs were co-transfected with empty vector (pcDNA) + mito-GFP (9:1) or pcDNA + ATP5A + mito-GFP (4.5:4.5:1), or pcDNA + ATP5B + mito-GFP (4.5:4.5:1) or ATP5A + ATP5B + mito-GFP (4.5:4.5:1). 48 h after transfection, the cells were fixed and GFP-mitochondria were imaged using a Leica 710 confocal microscope (upper panel).

Received: June 13, 2012

Published online: August 21, 2012

**Keywords:** ATP synthase · drug design · mitochondrial fusion · phenotypic screening

- [1] S. Hoppins, L. Lackner, J. Nunnari, *Annu. Rev. Biochem.* **2007**, *76*, 751–780.
- [2] D. C. Chan, *Annu. Rev. Cell Dev. Biol.* **2006**, *22*, 79–99.
- [3] a) A. B. Knott, G. Perkins, R. Schwarzenbacher, E. Bossy-Wetzel, *Nat. Rev. Neurosci.* **2008**, *9*, 505–518; b) M. Liesa, M. Palacin, A. Zorzano, *Physiol. Rev.* **2009**, *89*, 799–845; c) W. Liu, R. Acin-Perez, K. D. Geghman, G. Manfredi, B. Lu, C. Li, *Proc. Natl. Acad. Sci. USA* **2011**, *108*, 12920–12924; d) W. Yu, Y. Sun, S. Guo, B. Lu, *Hum. Mol. Genet.* **2011**, *20*, 3227–3240; e) M. Manczak, M. J. Calkins, P. H. Reddy, *Hum. Mol. Genet.* **2011**, *20*, 2495–2509; f) U. Shirendeb, A. P. Reddy, M. Manczak, M. J. Calkins, P. Mao, D. A. Tagle, P. H. Reddy, *Hum. Mol. Genet.* **2011**, *20*, 1438–1455; g) H. Xiong, D. Wang, L. Chen, Y. S. Choo, H. Ma, C. Tang, K. Xia, W. Jiang, Z. Ronai, X. Zhuang, Z. Zhang, *J. Clin. Invest.* **2009**, *119*, 650–660.
- [4] a) J. Estaquier, D. Arnoult, *Cell Death Differ.* **2007**, *14*, 1086–1094; b) T. Landes, L. J. Emorine, D. Courilleau, M. Rojo, P. Belenguer, L. Arnaune-Pelloquin, *EMBO Rep.* **2010**, *11*, 459–465; c) C. Brooks, S. G. Cho, C. Y. Wang, T. Yang, Z. Dong, *Am. J. Physiol. Cell Physiol.* **2011**, *300*, C447–455; d) T. Landes, J. C. Martinou, *Biochim Biophys Acta* **2011**, *1813*, 540–545.
- [5] a) A. Cassidy-Stone, J. E. Chipuk, E. Ingberman, C. Song, C. Yoo, T. Kuwana, M. J. Kurth, J. T. Shaw, J. E. Hinshaw, D. R. Green, J. Nunnari, *Dev. Cell* **2008**, *14*, 193–204; b) H. Otera, C. Wang, M. M. Cleland, K. Setoguchi, S. Yokota, R. J. Youle, K. Mihara, *J. Cell Biol.* **2010**, *191*, 1141–1158; c) M. Neuspiel, R. Zunino, S. Gangaraju, P. Rippstein, H. McBride, *J. Biol. Chem.* **2005**, *280*, 25060–25070; d) A. Olichon, L. Baricault, N. Gas, E. Guillou, A. Valette, P. Belenguer, G. Lenaers, *J. Biol. Chem.* **2003**, *278*, 7743–7746; e) R. Sugioka, S. Shimizu, Y. Tsujimoto, *J. Biol. Chem.* **2004**, *279*, 52726–52734.
- [6] F. Malka, O. Guillery, C. Cifuentes-Diaz, E. Guillou, P. Belenguer, A. Lombes, M. Rojo, *EMBO Rep.* **2005**, *6*, 853–859.
- [7] a) V. P. Skulachev, *Trends Biochem. Sci.* **2001**, *26*, 23–29; b) D. Tondera, S. Grandemange, A. Jourdain, M. Karbowski, Y. Mattenberger, S. Herzig, S. Da Cruz, P. Clerc, I. Raschke, C. Merkwirth, S. Ehses, F. Krause, D. C. Chan, C. Alexander, C. Bauer, R. Youle, T. Langer, J. C. Martinou, *EMBO J.* **2009**, *28*, 1589–1600; c) G. Twig, A. Elorza, A. J. Molina, H. Mohamed, J. D. Wikstrom, G. Walzer, L. Stiles, S. E. Haigh, S. Katz, G. Las, J. Alroy, M. Wu, B. F. Py, J. Yuan, J. T. Deeney, B. E. Corkey, O. S. Shirihai, *EMBO J.* **2008**, *27*, 433–446.
- [8] H. Chen, A. Chomyn, D. C. Chan, *J. Biol. Chem.* **2005**, *280*, 26185–26192.
- [9] Y. Zhang, D. C. Chan, *FEBS Lett.* **2007**, *581*, 2168–2173.
- [10] N. B. Gilula, M. L. Epstein, W. H. Beers, *J. Cell Biol.* **1978**, *78*, 58–75.
- [11] H. Chen, J. M. McCaffery, D. C. Chan, *Cell* **2007**, *130*, 548–562.
- [12] a) R. D. Phair, T. Misteli, *Nature* **2000**, *404*, 604–609; b) A. Tanaka, M. M. Cleland, S. Xu, D. P. Narendra, D. F. Suen, M. Karbowski, R. J. Youle, *J. Cell Biol.* **2010**, *191*, 1367–1380.
- [13] H. W. Platta, R. Erdmann, *FEBS Lett.* **2007**, *581*, 2811–2819.
- [14] a) M. Liesa, B. Borda-d'Agua, G. Medina-Gomez, C. J. Lelliott, J. C. Paz, M. Rojo, M. Palacin, A. Vidal-Puig, A. Zorzano, *PLoS one* **2008**, *3*, e3613; b) A. Wagatsuma, N. Kotake, K. Mabuchi, S. Yamada, *J. Physiol. Biochem.* **2011**, *67*, 359–370; c) A. Zorzano, M. I. Hernandez-Alvarez, M. Palacin, G. Mingrone, *Biochim. Biophys. Acta Bioenerg.* **2010**, *1797*, 1028–1033.
- [15] a) A. Tzagoloff, *J. Biol. Chem.* **1970**, *245*, 1545–1551; b) L. Lefebvre-Legendre, A. Balguerie, S. Duvezin-Caubet, M. F. Giraud, P. P. Slonimski, J. P. Di Rago, *Mol. Microbiol.* **2003**, *47*, 1329–1339.
- [16] A. I. Jonckheere, M. Huigsloot, M. Lammens, J. Jansen, L. P. van den Heuvel, U. Spiekerkoetter, J. C. von Kleist-Retzow, M. Forkink, W. J. Koopman, R. Szklarczyk, M. A. Huynen, J. A. Franssen, J. A. Smeitink, R. J. Rodenburg, *Mitochondrion* **2011**, *11*, 954–963.
- [17] a) A. E. Lang, A. M. Lozano, *N. Engl. J. Med.* **1998**, *339*, 1130–1143; b) X. Wang, B. Su, W. Liu, X. He, Y. Gao, R. J. Castellani, G. Perry, M. A. Smith, X. Zhu, *Aging Cell* **2011**, *10*, 807–823.
- [18] a) D. G. Breckenridge, M. Stojanovic, R. C. Marcellus, G. C. Shore, *J. Cell Biol.* **2003**, *160*, 1115–1127; b) S. Frank, B. Gaume, E. S. Bergmann-Leitner, W. W. Leitner, E. G. Robert, F. Catez, C. L. Smith, R. J. Youle, *Dev. Cell* **2001**, *1*, 515–525.